JOURNAL OF VIROLOGY, Jan. 2005, p. 1053–1061 Vol. 79, No. 2
0022-538X/05/$08.00+0 doi:10.1128/JVI.79.2.1053–1061.2005
Copyright © 2005, American Society for Microbiology. All Rights Reserved.

Deletion of Penton RGD Motifs Affects the Efficiency of both the Internalization and the Endosome Escape of Viral Particles Containing Adenovirus Serotype 5 or 35 Fiber Knobs

Dmitry M. Shayakhmetov,[1]† Andrea M. Eberly,[1]† Zong-Yi Li,[1] and André Lieber[1,2]*

Department of Medicine[1] and Department of Pathology,[2] University of Washington School of Medicine, Seattle, Washington

Received 17 June 2004/Accepted 3 September 2004

Adenovirus (Ad) vectors are widely used for gene delivery in vitro and in vivo. A solid understanding of the biology of this virus is imperative for the development of novel, effective, and safe vectors. For the group C adenovirus serotypes 2 and 5 that use CAR as a primary attachment receptor, it is known that the penton base RGD motifs interact with cellular integrins and that this interaction promotes virus internalization. However, the RGD motif's impact on the efficiency of postinternalization steps, such as the escape of the virus particle from the endosome, is less defined. Furthermore, the role of penton-integrin interactions remains unknown for new vectors possessing group B Ad fiber knobs that use CD46 as a primary virus attachment receptor. In this study, we used vectors with the RGD motif deleted that contained Ad5 and B-group Ad35 fiber knobs and long fiber shafts and studied the role of RGD-integrin interactions in virus internalization and endosome escape. The deletion of the RGD motif in the penton base did not affect virus attachment, regardless of the type of cellular receptor used for attachment. RGD motif deletion, however, significantly reduced the rate of virus internalization for both the Ad5 and Ad35 fiber knob-containing vectors. This study also demonstrates the role of penton RGD motifs in facilitating the endosome escape step of virus infection and indicates that penton-integrin interactions are involved in internalization of capsid-chimeric CD46-interacting Ads with long fiber shafts.

The vast majority of currently used adenovirus (Ad) vectors are based on serotype 5 (Ad5). In vitro, Ad5 uses a two-step mechanism to infect cells. The first step is a high-affinity interaction between the Ad fiber knob and the coxsackie-adenovirus receptor (CAR) (28), which requires a flexible, long (22 β-repeats) fiber shaft (36, 39, 44, 48). Following initial attachment, RGD motifs within the Ad5 penton base interact with cellular integrins, including αvβ1, αvβ3, αvβ5, αvβ6, α5β1, $\alpha_M\beta2$, $\alpha_L\beta2$ (7, 8, 13, 16, 21, 46). Interaction with integrins initiates signaling (through phosphatidylinositol-3-kinase/mitogen-activate protein kinase (MAPK) and Raf1/ERK1/2 pathways), resulting in actin polymerization near the site of virus attachment triggering endocytosis via clathrin-coated pits (18). Apparently CAR functions only as a dock for the capsid to bring it close to integrins, and no CAR-mediated signaling is required for efficient virus internalization or trafficking. Upon endocytosis, the intra-endosomal pH drops due to acidification by proton pumps. At pH 6.0, the virus penetrates the endosomal membrane and escapes to the cytosol, thus evading degradation by lysosomal enzymes. The endosomalytic activity of the virus is attributed to the penton, as studies show that the penton undergoes a conformational change at low pH, exposing hydrophobic regions that bind nonionic detergents (20). Moreover, a blocking antibody against the penton inhibits endosome escape. At low pH, the virus penton is bound to integrins, which enables escape to the cytosol (1). The critical role of interactions between penton RGD motifs and αvβ5 integrins for efficient virus infection has been demonstrated in studies with Ads in which RGD has been deleted or mutated (1). These interactions also activate signaling that involves protein kinase C (PKC), which is required for endosomal lysis (20). Finally, the Ad protease greatly influences viral cell entry and endosome escape. The protease is packaged into the capsid and inactivated after capsid release from the cell (into an oxidizing environment) but reactivated after virus entry into acidified endosomes (20). Upon release into the cytoplasm, viral particles engage in bidirectional movement along microtubules (19, 40), ultimately leading to the docking of partially disassembled capsids with nuclear pore complexes and the translocation of viral genomes into the nucleus.

The efficiency of Ad5 infection depends on the levels of CAR and integrin expression. However, many potential gene therapy targets, such as hematopoietic stem cells, dendritic cells, endothelial cells, and malignant tumor cells express only low levels of CAR and/or integrins, rendering them relatively resistant to infection by Ad5-based vectors (17, 27, 43, 47). Chimeric Ad5 vectors possessing fiber proteins derived from human subgroup B Ad serotypes such as Ad11, Ad16, Ad35, or Ad50 have become increasingly popular as gene transfer vectors because they can efficiently deliver genes to cell types that are refractory to Ad5 infection (10, 24, 29, 31, 34, 37, 45). Recently, we and others demonstrated that most group B Ads, as well as one member of group D (Ad37), utilize CD46 as a high-affinity primary attachment receptor (9, 30, 38, 49). Binding of chimeric Ad5-based vectors possessing group B Ad35 or Ad7 fibers to cellular attachment receptor(s) was found to predetermine incoming virus particles to an intracellular trafficking route that is different from that of unmodified Ad5

* Corresponding author. Mailing address: Department of Medicine, University of Washington School of Medicine, Seattle, WA 98195. Phone: (206) 221-3973. Fax: (206) 685-8675. E-mail: lieber00@u.washington.edu.

† D.M.S. and A.M.E. contributed equally to this work.

vectors (22, 23, 35). While Ad5 efficiently escaped from the endosomal environment early after infection, Ad particles with Ad35 fibers or fiber knobs remained in late endosomal or lysosomal compartments and used these compartments to achieve localization to the nucleus. However, a significant number of these particles appeared to be retrogradely transported and deposited at the cell surface.

CD46 is used by other pathogens as a cellular receptor. However, all other viruses that bind to CD46 are enveloped viruses: either RNA viruses (measles virus, bovine viral diarrhea virus) or enveloped DNA viruses (human herpesvirus 6). These viruses enter the cell via fusion with the plasma membrane. It is currently unclear whether the nonenveloped B-group Ads use CD46 for internalization or whether this requires coreceptor(s), such as integrins. B-group Ads 3, 35, and 11 possess RGD motifs in their penton base, and the same is true for chimeric Ad5/11 and Ad5/35, which possess Ad5 pentons.

In this study, we utilized Ad vectors with the penton base RGD motif deleted to study the role of Ad-cellular integrin interactions in postattachment steps of virus infection. We found that for both CAR- and CD46-interacting vectors, deletion of the RGD motif in the penton base dramatically reduces the rate of virus particle internalization into cells. Moreover, we found that RGD motif-dependent interactions with cellular integrins support efficient virus escape from endosomes.

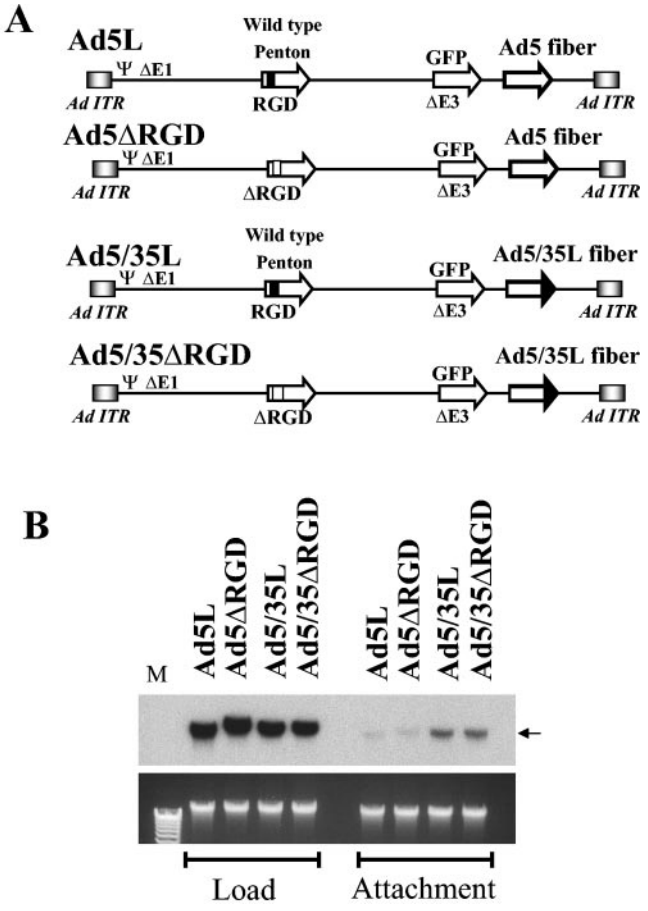

FIG. 1. (A) Schematic representation of genome organizations of fiber chimeric Ad vectors possessing wild-type or mutant penton proteins with the RGD motif deleted. (B) Comparative analysis of Ad vector attachment to A549 cells. (Upper panel) Equal amounts of indicated Ad vectors were mixed with A549 cells, and one portion of cells was lysed immediately (Load lanes), while the others were processed to determine the levels of Ad attachment (Attachment lanes) by Southern blotting as described in Materials and Methods. The lower panel shows the agarose gel before Southern blotting to demonstrate equivalent DNA loads. The membrane was hybridized with a GFP gene-specific ^{32}P-labeled probe, and vector DNA was visualized by autoradiography. M, molecular weight marker. Corresponding vector DNA bands are indicated by arrows.

MATERIALS AND METHODS

Cells and viruses. HeLa cells (human cervix carcinoma, ATCC CCL-2.2), 293 (human embryonic kidney; Microbix, Toronto Canada), A549 cells (human lung carcinoma, ATCC CCL-185, and AE25 cells (Ad E1A-expressing A549 cells) (4) were grown in DMEM, supplemented with 10% fetal calf serum (FCS), 2 mM L-glutamine and 1× penicillin-streptomycin solution (Invitrogen, Carlsbad, Calif.). Human leukemic cells of line MO7e (17) were maintained in RPMI 1640 medium containing 10% FCS, 2 mM L-glutamine, 100-U/ml penicillin, 100-μg/ml streptomycin, and 0.1-ng/ml granulocyte-macrophage colony-stimulating factor (Immunex, Seattle, Wash.). The viruses Ad5L and Ad5/35L, expressing green fluorescent protein (GFP) under the control of the human cytomegalovirus immediate-early promoter, were previously constructed and are described in detail elsewhere (36). Ad5ΔRGD and Ad5/35ΔRGD were constructed by standard cloning techniques and DNA recombination in *Escherichia coli* strain BJ5183 (6). The genomes of Ad5L and Ad5/35L (in the corresponding plasmids pAd5L and pAd5/35L) were linearized with FseI endonuclease and recombined with the Ad penton-encoding sequence derived from plasmid pB21ΔRGD (kindly provided by V. Krasnykh, M. D. Anderson Cancer Center, Houston, Tex). pB21ΔRGD possesses a deletion of the RGD amino acid residues within the Ad penton sequence. Following homologous recombination in *E. coli*, the plasmids pAd5ΔRGD and pAd5/35ΔRGD were generated and corresponding viruses were rescued in 293 cells as described earlier (37). Deletion of the RGD motif in the penton base gene was confirmed by PCR analysis and by direct sequencing of the penton coding sequence, using viral genomes as a template. All viruses were amplified in 293 cells under conditions preventing cross-contamination. Viruses were banded in CsCl gradients; viral bands were collected, dialyzed, and aliquoted as described elsewhere (5). Ad genome concentrations were determined by both quantitative Southern blotting and plaque-forming assays on 293 cells. For quantitative Southern blot analysis, DNA was extracted from purified viral particles and was run on agarose gels in serial (twofold) dilutions together with standard DNA of known concentrations (preparatively purified Ad5L DNA). After transfer onto Hybond N+ nylon membranes (Amersham, Piscataway, N.J.), filters were hybridized with a ^{32}P-labeled DNA probe (0.7-kb fragment, corresponding to the GFP gene of pEGFP-1, Clontech, Palo Alto, Calif.) and DNA concentrations were measured by PhosphorImager. These values were used to calculate the genome titer for each virus stock used. For each Ad vector used in this study, at least two independent virus stocks were produced and characterized by PFU titering on 293 cells and genome titering by Southern blotting.

Analysis of Ad attachment to cells. Studies of the analysis of Ad attachment to cells were based on a protocol published elsewhere (36). For attachment studies, 3.5×10^5 A549 cells were incubated for 1 h on ice with equal amounts of Ad particles, corresponding to a multiplicity of infection (MOI) of 8,000 virions per cell, in 100 μl of ice-cold adhesion buffer (DMEM supplemented with 2 mM $MgCl_2$, 1% bovine serum albumin, 20 mM HEPES). Cells were then pelleted by centrifugation at $1,000 \times g$ for 4 min and washed two times with 0.5 ml of ice-cold phosphate-buffered saline (PBS). After the last washing step, the cells were pelleted at $1,500 \times g$, the supernatant was removed, cells were lysed, and total cellular DNA was extracted as described previously (36). To ensure equivalent viral loads (Load lanes in Fig. 1B), following virus addition, cells were immediately lysed and cellular DNA was extracted for subsequent Southern blot analysis as described above.

Ad internalization rate analysis. Briefly, 2×10^5 A549, HeLa, or MO7e cells were resuspended in 150 μl of adhesion buffer (DMEM supplemented with 2 mM $MgCl_2$, 1% bovine serum albumin, 20 mM HEPES) and chilled for 25 min on ice. Then the cells were further incubated on ice for 1 h with equal amounts of Ad particles at an MOI of 1,000 virus particles per cell. Next, unattached virus particles were removed and cells were washed twice with 200 μl of ice-cold PBS. Following the last wash, cells were resuspended in PBS and transferred to a 37°C water bath to initiate virus internalization. At the indicated time points, 20 μl of polyclonal anti-Ad5 antibody was added to the cells to neutralize noninternalized

virus particles. In the control settings, no anti-Ad antibody was added to cells in order to determine the maximum levels of cell transduction for each virus (taken as 100%). To complete neutralization of noninternalized vector particles, after addition of anti-Ad5 antibody, cells were further incubated on ice for 30 min. Then, they were washed twice with PBS and plated in 1 ml of growth medium onto 12-well plates and incubated overnight at 37°C. Both the percentage of cells expressing virus-encoded GFP and the mean GFP fluorescence intensity were determined by flow cytometry. Due to the low attachment efficiency of Ad5L and Ad5ΔRGD vectors to MO7e cells, for infection of these cells, 10 times higher MOIs of Ad5L and Ad5ΔRGD vectors were used compared to those of the Ad5/35L and Ad5/35ΔRGD vectors.

Labeling of Ads with Cy3 fluorochrome. To label Ad capsids with Cy3 (red) fluorochrome (Cy3 Bifunctional Reactive Dyes; Amersham Pharmacia Biotech, United Kingdom), we used the manufacturer's protocol without modifications. The ratio between the volumes of Ad and labeling reagent was 1/9. Labeled viruses were dialyzed against 10 mM Tris-HCl, pH 7.5, 10 mM $MgCl_2$, and 10% glycerol solution at 4°C overnight to remove unincorporated chemicals. The concentrations of dye-labeled viruses were determined by quantitative Southern blotting as described above.

Flow cytometry. MO7e, HeLa, or A549 cells (2×10^5 per sample) were stained in triplicate with primary mouse monoclonal antihuman αv, α4, α5, αvβ5, αvβ3, and β3 antibodies (all from BD Biosciences Pharmingen, San Diego, Calif.) for 1 h on ice. Then the cells were washed, and specific binding of primary antibodies was developed with secondary, phycoerythrin-conjugated antimouse secondary antibody. Following 30 min of incubation, cells were washed and analyzed by flow cytometry. As a negative control, the indicated cell lines were stained with secondary antibody only.

Analysis of intracellular Ad trafficking. HeLa cells (5×10^4) or A549 cells (4×10^4) were seeded into eight-chamber glass slides in standard growth media 1 day prior to infection. The following day, cells were washed with PBS and incubated on ice for 15 min. Virus particles labeled with Cy3 were added at a concentration of 6×10^9 particles per ml of culture medium. After incubation at 37°C for 15 min, the virus-containing medium was removed and new growth medium was added. The cells were incubated for the indicated times before being fixed with a mixture of methanol and acetone (1:1 [vol/vol]). In order to analyze Ad attachment, one slide was immediately washed with cold PBS after the 15-min incubation time and fixed. For analysis of intracellular virus distribution and virus colocalization with endosomal or lysosomal cellular compartments, fixed cells were incubated with the polyclonal rabbit anti-cathepsin B antibody Ab-3 (Oncogene, Boston, Mass.) (1/20 dilution) at 37°C for 1 h. Alexafluor-488-conjugated goat anti-rabbit secondary antibody (Molecular Probes, Eugene, Oreg.) (1/200 dilution) was used to develop the binding of the primary antibody for 30 min at room temperature. The cells were then visualized with a Leica fluorescent microscope and Leica spectral confocal microscope.

Ad endosome escape inhibition assay. This assay is based on a previously published study (22). A549 cell-derived AE25 cells (5×10^5) were seeded onto six-well plates 2 days prior to the experiment. Following the results from the internalization rate experiment, it was known that the variants with RGD deleted internalized at a lower rate. To determine how much more Ad5/35ΔRGD and Ad5ΔRGD needed to be applied to cells in order to have comparable numbers of infectious virus enter the cell, a preliminary study was done comparing two fixed concentrations of RGD-possessing viruses to four concentrations of vector with the RGD motif deleted. At the day of experiment, cells (grown to a density of 2×10^6 per well) were chilled at 4°C for 45 min. Then viruses diluted in 1 ml of ice-cold DMEM (500 and 1,000 particles/ml per well for both Ad5L and Ad5/35L and 2,000, 4,000, 6,000, 8,000, and 10,000 particles/ml per well for both Ad5ΔRGD and Ad5/35ΔRGD) were applied to cells and allowed to attach to cells for 1 h. Medium with nonattached virus particles was then removed, and the virus infection was initiated by transferring cells into a 37°C water bath. Five minutes postinitiation of virus infection, 110 μl of anti-Ad5 antibody (see above) was added to the media in order to block further internalization of Ad particles. Cells were then left at 37°C for another 2 h before being overlaid with 3 ml of overlay medium (minimal Earls medium, 10% fetal bovine serum, 2 mM L-glutamine, 0.5% agarose). On the 4th day after the first overlay, an additional 1 ml of overlay medium was added to cells. Plaques were counted 10 days postinfection. In order to block the escape of virus from endosomes, a 50 mM solution of NH_4Cl was used. Cells were infected with Ads as described above (MOIs of 2,000 and 20,000 particles/ml for Ad5L and Ad5ΔRGD and MOIs of 1,000 and 10,000 particles/ml for Ad5/35L and Ad5/35ΔRGD, respectively). At 5 min postinitiation of virus infection, medium was removed and DMEM containing anti-Ad5 antibody was added to cells. At 15, 30, and 60 min postinitiation of virus infection, 1 ml of 100 mM NH_4Cl in growth medium was added to cells to bring the final concentration of NH_4Cl in each well to 50 mM. Following drug addition, cells were incubated for another 2 h before being rinsed and overlaid as above. Plaques were counted on day 10 after infection. In the control settings, no NH_4Cl was added to cells to determine the efficiency of cell infection for each experiment. All infections were done in duplicate. The figures show representative data obtained from three to five independent experiments.

RESULTS

Penton RGD motif deletion does not affect the initial attachment step of infection for CAR- or CD46-interacting adenoviruses. Previous studies have demonstrated that Ad interaction with cellular integrins facilitates internalization of CAR-interacting Ad2 and Ad5 viruses into the cell following the primary attachment event (46). However, the role of these interactions in postinternalization steps of infection as well as in cell infection by non-CAR-interacting viruses and capsid-chimeric vectors remains unclear. To analyze the role of Ad-integrin interactions in early steps of infection for wild-type and B-group fiber-containing Ads, we utilized the previously constructed first-generation E1/E3-deleted Ad5-based vectors with unmodified (Ad5L) or chimeric (Ad5/35L) fibers (36). Ad5/35L is identical to Ad5L; however, it possesses the group B Ad35-derived fiber knob domain recognizing CD46 as a primary attachment receptor (9). Our previous studies showed that substituting the Ad fiber knob domain from Ad5 to Ad35 was sufficient to change the intracellular trafficking route of internalized virus particles (36). Because the effect of fiber shaft length on virus-integrin interactions is still unknown, in this study, we used only Ad vectors with identical long Ad5-derived fiber shaft domains. In Ad5ΔRGD and Ad5/35ΔRGD (Fig. 1A), the sequence encoding the RGD motif within the penton base protein was deleted via PCR-directed mutagenesis. To confirm that the RGD deletion did not reduce the ability of Ads to interact with the primary virus attachment receptors, we analyzed the efficiency of virus attachment to A549 cells by Southern blot analysis. This analysis revealed that when cells were exposed to equivalent doses of viral vectors (Fig. 1B, Load lanes), significantly more Ad5/35L and Ad5/35ΔRGD particles attached to cells, compared to Ad5L and Ad5ΔRGD vectors (Fig. 1B, Attachment lanes). This is not surprising considering the up-regulation of CD46 on tumor cell lines (12, 14, 25, 42). Importantly, Ad vectors with the RGD motif deleted attached to cells as efficiently as the vectors possessing intact pentons in their capsids.

To better understand the role of Ad-integrin interactions in early steps of Ad infection, we utilized three cell lines, MO7e, A549, and HeLa, which express different levels and types of integrins. Immunohistochemical staining revealed (Fig. 2) that while all of these cells express high levels of αv integrins, only A549 and HeLa express significant levels of αvβ5 integrins. In contrast, MO7e cells express higher levels of αvβ3 integrins than the other cell lines. We found that all cell lines tested express low levels of α4, α5, and β3 integrins. The analysis of vector infectivity on these cell lines demonstrated that, in agreement with the virus attachment data, Ad35 fiber knob-possessing vectors are superior at transducing all transformed cell lines tested compared to vectors possessing unmodified Ad5 fibers (Fig. 3). Although for CAR-interacting Ad5L and Ad5ΔRGD vectors, the deletion of RGD motif within the penton protein did not significantly affect their ability to transduce cells, Ad5/35ΔRGD demonstrated a slight, but statisti-

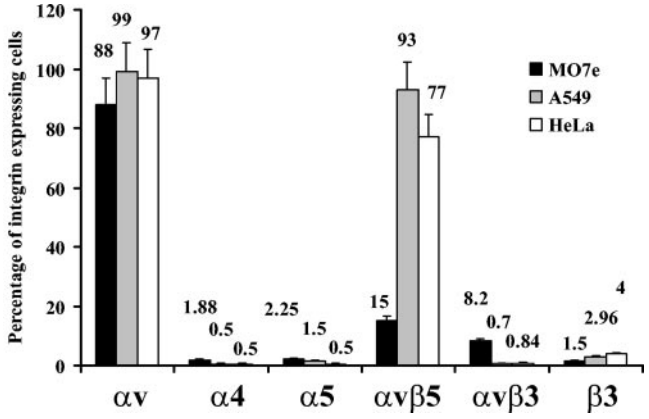

FIG. 2. Immunohistochemical analysis of the levels of integrin expression on MO7e, A549, and HeLa cells. The mean percentage of positively stained cells is indicated next to the corresponding column. Error bars indicate standard deviations.

cally significant ($P < 0.05$) reduction in infectivity compared to Ad5/35L. Taken together, these data demonstrate that deletion of the penton RGD motifs does not affect the initial attachment step of infection for both CAR- and CD46-interacting Ads. However, deletion of the RGD motif reduces the overall infectivity of capsid-modified CD46-interacting vectors to a greater degree than their CAR-interacting counterparts.

Adenoviruses with deleted RGD motifs demonstrate slower internalization into cells compared to unmodified vectors. In our earlier studies, the comparative analysis of infection inhibition for Ad5 and capsid-modified Ad5/35 vectors on human erythroleukemia K562 cells using anti-αv-integrin antibodies demonstrated only a modest decline in infectivity (37). These data suggested that, unlike Ad5 vectors, which utilize CAR and αv-integrins for their attachment to and internalization into the cell, vectors recognizing receptors different from CAR might not require interaction with cellular integrins for efficient internalization. On the other hand, different cell types express different integrins, and recently it has been shown that Ad5 can use other integrins (such as α5β1, α3β1, α_{IIM}, etc.) in addition to $\alpha v\beta_3/\beta_5$ integrins (7, 8, 13, 16, 21, 46). To evaluate

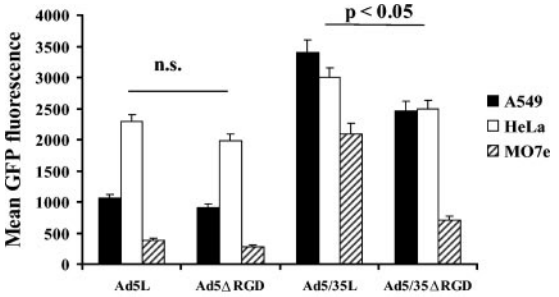

FIG. 3. Transduction efficiency of different cell lines with Ad vectors possessing wild-type pentons and pentons with the RGD motif deleted. A549, HeLa, and MO7e cells were infected at an MOI of 1,000 virus particles per cell, and the mean GFP fluorescent intensity was analyzed 24 h later by flow cytometry. $n = 6$. n.s., statistically nonsignificant. Note that for each individual cell line tested, the efficiency of cell infection with Ad5/35ΔRGD vector was significantly lower than that with Ad5/35L ($P < 0.05$).

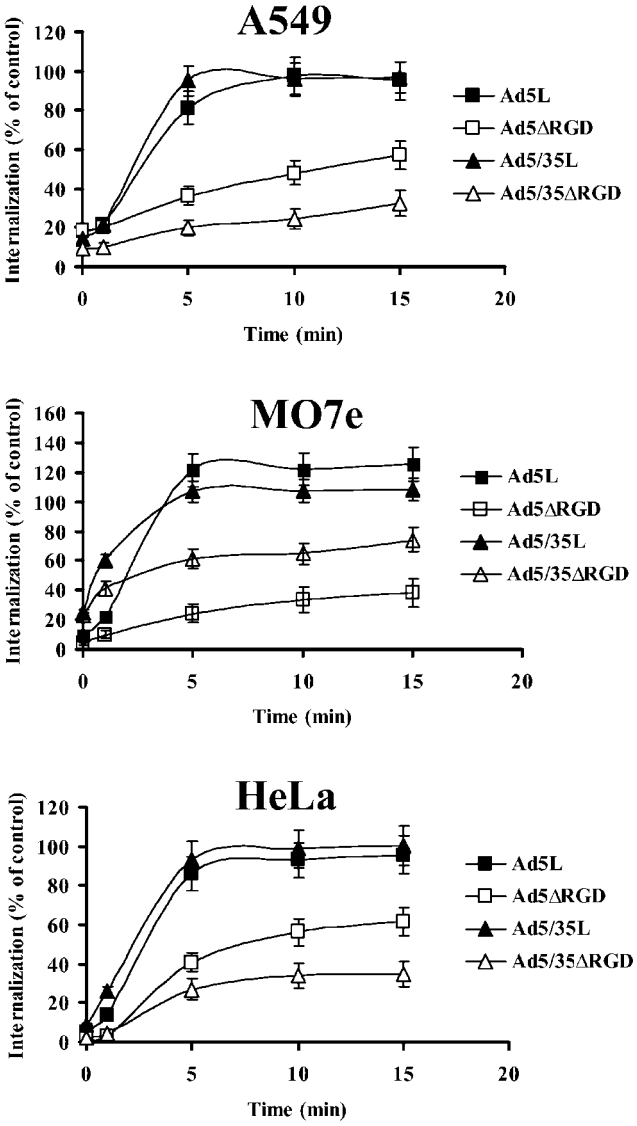

FIG. 4. Effect of the RGD motif deletion on the rates of internalization of Ad vectors. Virus vectors were allowed to attach to A549, MO7e, and HeLa cells on ice as described in Materials and Methods. Infection was initiated by cell transfer to 37°C. At indicated time points, an anti-Ad5 neutralizing antibody was added to cells to prevent further internalization of infectious particles. The resultant levels of gene transfer (as a mean of GFP fluorescence intensity) was assessed by flow cytometry 24 h postinfection. The level of infection for each virus when no virus-neutralizing antibody was added (control settings) was taken as 100%. All infections were done in triplicate, and the data presented are representative of two independent experiments.

whether RGD-mediated interactions with integrins are ultimately required for both CAR-interacting (Ad5 fiber knob domain) and CD46-interacting (Ad35 fiber knob domain) vectors, we infected A549, HeLa, and MO7e cells with vectors possessing wild-type pentons or pentons with the RGD motif deleted and analyzed the kinetics of their internalization into cells (Fig. 4). This analysis revealed that both CAR-interacting and CD46-interacting vectors with the RGD motif deleted demonstrated drastically reduced rates of internalization into cells compared to their corresponding controls. On all cell lines

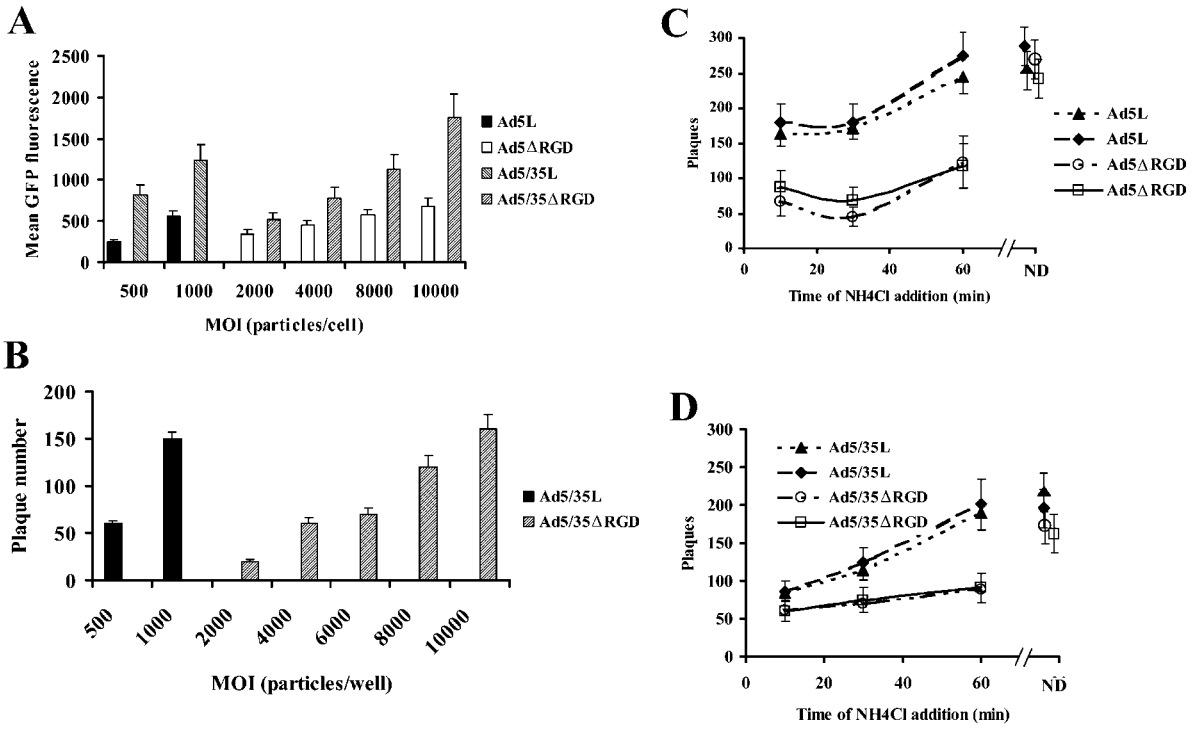

FIG. 5. Effect of the RGD motif deletion on the rate of endosome escape of Ad vectors. MOIs of vectors with the RGD motif deleted, allowing for gene transfer levels comparable to those of variants possessing the RGD motif by flow cytometry (A) and plaque assay (B), were determined. At indicated MOIs, viruses were allowed to attach to AE25 cells on ice for 1 h. Unattached virions were removed and infection was initiated by cell transfer to 37°C. Five minutes later, anti-Ad-neutralizing antibody was added to cells to prevent further internalization of infectious virus particles. The levels of gene transfer were assessed 24 h postinfection and 10 days postinfection (by flow cytometry and plaque assay, respectively). Determination of the rate of endosome escape for different vectors possessing the RGD motif or with the RGD motif deleted (C and D). AE25 cells (2×10^6 per well) in six-well plates were infected with Ads as described above, and at 15, 30, and 60 min postinitiation of virus infection, ammonium chloride was added to the medium to prevent acidification of cellular endosomes. Cells were incubated with the drug for 2 more h and then were washed and overlaid with agarose-containing medium. The number of plaques in monolayers of cells was counted 10 days postinfection. Cells were infected with Ad-containing medium at concentrations of 2,000 and 20,000 particles/ml for Ad5L and Ad5ΔRGD and at concentrations of 1,000 and 10,000 particles/ml for Ad5/35L and Ad5/35ΔRGD, respectively. Therefore, the MOI did not exceed 0.01 virus particle per cell. The graphs show the data obtained in two independent experiments, performed in duplicate. In the control setting, no ammonium chloride was added to the cells. ND, no drug.

studied, 80 to 100% of Ad5L and Ad5/35L vectors were internalized into cells by 5 min postinitiation of internalization. In contrast, only 20 to 40% of vectors with RGD deleted were internalized into cells by this time. Although by 10 and 15 min postinitiation of internalization the proportion of internalized vectors with the RGD motif deleted increased compared to earlier time points, their levels did not exceed 60% of internalization for the RGD-possessing vectors, and the overall internalization kinetics were dramatically slower than those for the Ad5L and Ad5/35L vectors. These data demonstrate that although different integrins may be involved in facilitating internalization of wild-type or capsid-modified Ads into analyzed cell lines, independently of the nature of the primary attachment receptor (CAR or CD46), Ads require RGD-mediated interactions with integrins for efficient internalization into cells.

Intracellular trafficking and the endosome escape step of infection are affected by the deletion of the penton RGD motifs. To analyze whether deletion of the RGD motif within the Ad penton base may affect the efficiency of postinternalization steps of virus infection (specifically, the endosomal escape) we utilized a plaque-forming inhibition assay on AE25 cells (4). AE25 is a cell line derived from A549 cells that stably expressed Ad E1a to complement replication of first-generation vectors with E1/E3 deletions. AE25 cells also maintain high viability upon exposure to ice-cold media during virus attachment and subsequent overlay with agar-containing media, required for the plaque assay. In preliminary experiments, we found that monolayers derived from other cell lines, such as HEK293 or HeLa, readily disintegrate under these conditions.

Earlier studies with Ad2 (CAR interacting) have shown that about 50% of particles escape from endosomes by 15 min post-virus internalization (11, 15), and our data showed that vectors with the RGD motif deleted demonstrated slowed internalization kinetics. To assess the rate of endosome escape for different vectors, we first had to equalize the number of infectious wild-type vector particles and vector particles with the RGD motif deleted that enter the cell in a synchronized manner. To do this, we allowed attachment on ice of wild-type vectors and increasing MOIs of their counterparts with the RGD motif deleted. Following removal of unattached virus particles and initiation of internalization by transfer of cells to 37°C for 5 min, Ad-neutralizing antibodies were added to cells. Later, the levels of cell transduction based on GFP expression or the number of formed plaques for different vectors (Fig. 5A and B) was analyzed as described in Materials and Methods.

These studies revealed that, compared to RDG motif-possessing viruses, roughly 10 times more of the doses of vectors with the RGD motif deleted were needed under these conditions to achieve gene transfer levels comparable to those of wild-type penton-containing Ads.

To compare the kinetics of endosome escape of vectors possessing the RGD motif with those with the RGD motif deleted, we used an endosomal pH neutralization plaque assay. Ads were allowed to attach to and internalize into cells for 5 min prior to neutralization with antibodies as described above. At different times post anti-Ad antibody addition, cells were incubated with 50 mM ammonium chloride-containing medium to prevent acidification of cellular endosomes. Subsequently, cells were incubated for another 2 h at 37°C. Following this incubation, the ammonium chloride-containing medium was removed, cells were overlaid with growth medium supplemented with 0.5% agarose, and plaques formed in cellular monolayers by 10 days post-virus infection were counted (Fig. 5C and D). This analysis revealed that when no ammonium chloride-containing medium was used, similar numbers of plaques were seen following cell infection with vectors possessing the RGD motif and vectors with the RGD motif deleted (MOIs of 1,500 and 15,000 virus particles per well, respectively). However, the addition of ammonium chloride-containing medium to cells 15 min postinitiation of virus internalization dramatically reduced the number of formed plaques for both wild-type vectors and those with the RGD motif deleted. The analysis of numbers of plaques formed following the addition of ammonium chloride-containing medium at 15, 30, and 60 min postinitiation of virus internalization revealed that the kinetics of virus escape from endosomes are significantly slower for vectors with the RGD motif deleted than for their wild-type counterparts. While cell infection with Ad5L virus could not be efficiently blocked by addition of ammonium chloride at 15 min postvirus internalization (more than 70% of virus particles have already escaped from endosomes by this time), the Ad5ΔRGD infection was still sensitive to ammonium chloride addition (Fig. 5C). Moreover, in contrast to Ad5L vector, the addition of ammonium chloride 15 min postvirus internalization efficiently blocked both Ad5/35L and Ad5/35ΔRGD infection (Fig. 5D). Again, the kinetics of Ad5/35ΔRGD endosome escape were apparently slower than those of Ad5/35L. For Ad5L, the time when 50% of virus escaped from the endosome based on our assay corresponded to 5 to 15 min post-virus internalization. For Ad5/35L, at least 30 min post-virus internalization was needed to allow 50% of virus to escape the neutralizing activity of ammonium chloride. Taken together, our data demonstrate that the deletion of the penton RGD motif reduced the efficiency of Ad escape from endosomes independently of whether CAR or CD46 was used for primary Ad attachment to the cells. Our data also demonstrate that the kinetics of endosome escape are slower for capsid-modified CD46-interacting vectors than those for their CAR-interacting counterparts.

The reduced rates of endosome escape for vectors with the RGD motif deleted should be reflected by altered intracellular trafficking of virus particles, compared to unmodified RGD motif-possessing controls. To assess the intracellular trafficking of vectors with the RGD motif deleted, we infected A549 cells with Ads labeled with fluorophore Cy3 (35). Our previous analyses revealed that the capsid-modified Ad5/35L vector, following initial binding to CD46, travels to the perinuclear space within the late endosomal/lysosomal cathepsin B-positive intracellular compartments (35). In contrast, CAR-interacting Ad5L vector rapidly escaped from endosomes and did not colocalize with cathepsin B-positive compartments during early times of virus infection. To analyze the intracellular trafficking of Cy3-labeled Ads, we pulse-infected A549 cells (grown on coverslips) with virus at an MOI of 10^4 virus particles per cell for 15 min at 37°C. Following this incubation, cells were washed to remove unattached particles and either immediately fixed or further incubated for the indicated times. Cells were then fixed and stained with anti-cathepsin B antibodies to analyze virus colocalization with late endosomal or lysosomal cellular compartments (Fig. 6). This analysis revealed that similarly to its trafficking in HeLa cells (36), CAR-interacting Ad5L vector did not colocalize efficiently with cathepsin B-positive intracellular compartments at the early time points of infection (up to 2 h). In contrast, Ad5/35L vector efficiently colocalized with cathepsin B-positive cellular compartments as early as 30 min postvirus infection. However, confocal microscopic analysis also revealed that the intracellular distributions of both vectors with the RGD motif deleted Ad5ΔRGD and Ad5/35ΔRGD vector did not match those of their counterparts possessing the RGD motif. While almost all Ad5L virus particles efficiently accumulated in the perinuclear space, forming characteristic red circles around the nuclear membrane by 30 and 60 min postvirus infection, more Ad5ΔRGD particles remained scattered in the cytoplasm at these times. This phenomenon was even more pronounced for CD46-interacting vectors. Although both Ad5/35L and Ad5/35ΔRGD vector particles rapidly entered cathepsin B-positive cellular compartments, the vector with the RGD motif deleted Ad5/35ΔRGD was clearly delayed at migrating to the perinuclear space. The majority of Ad5/35L virus particles reached the nucleus by 60 min postvirus infection. However, Ad5/35ΔRGD vector particles remained widely distributed throughout the cytoplasm (Fig. 6, compare Ad5/35L and Ad5/35ΔRGD, 60-min time point), and it required another hour for this virus to accumulate at the nuclear membrane with an efficiency comparable to that of Ad5/35L. In summary, our data demonstrate that penton base RGD motif deletion significantly reduced both the ability of Ad to escape from the endosome and intracellular trafficking, resulting in delayed virus accumulation at the nuclear membrane.

DISCUSSION

In this study, we compared internalization and endosome escape of Ad vectors that utilize different attachment receptors, CAR or CD46. To assess the involvement of penton-integrin interactions, the integrin-binding RGD motif within the pentons of these vectors was deleted. Our study revealed that both CAR-interacting and CD46-interacting vectors with the RGD motif deleted demonstrated reduced rates of internalization into cells compared to their RGD motif-containing counterparts. Furthermore, we found that penton base RGD motif deletion affected the ability of Ad particles to escape from endosomes, resulting in an altered pattern of intracellular trafficking and delayed delivery of viral particles to the nucleus.

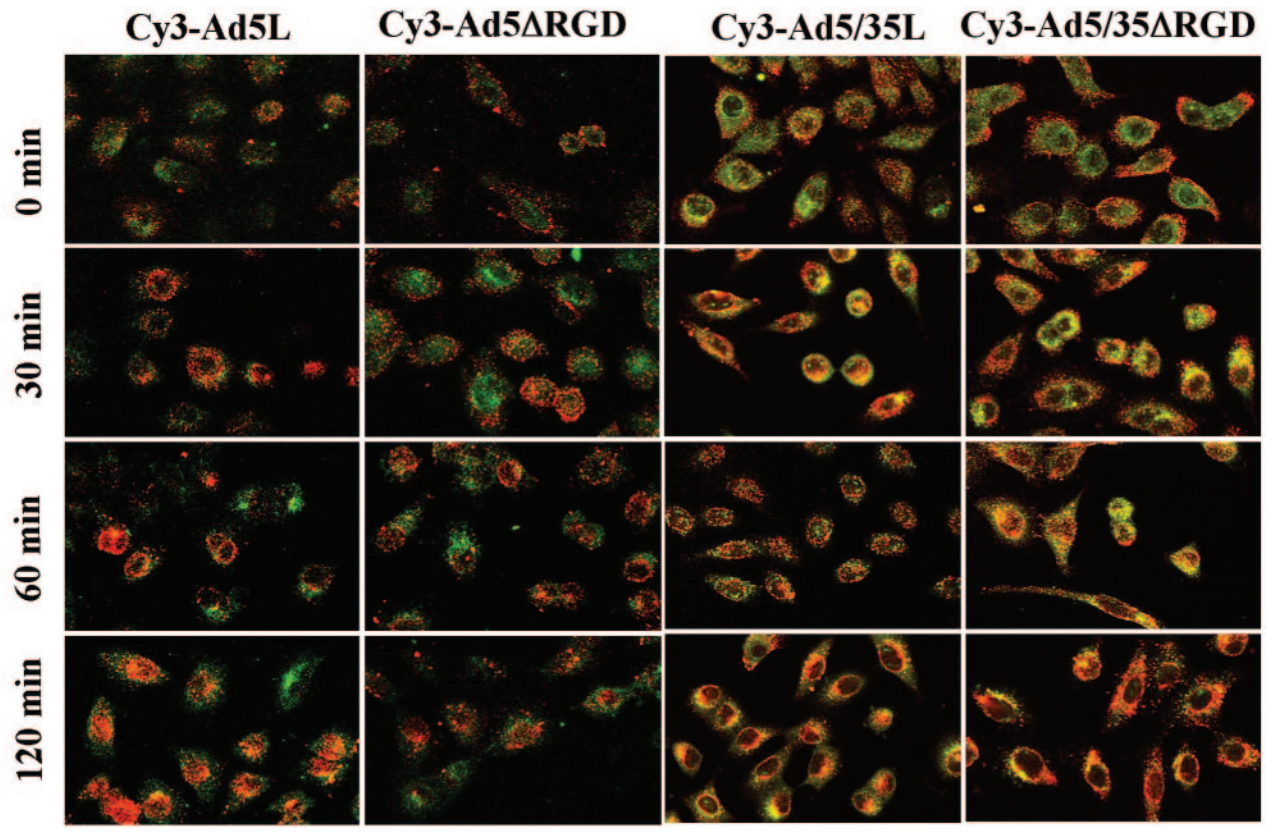

FIG. 6. Intracellular trafficking of Cy3-labeled Ad vectors in A549 cells. The kinetics of Cy3-labeled Ad vectors are shown in red, and colocalization with cathepsin B-containing late endosomal or lysosomal cellular compartments is shown in green. Cells were pulse-infected with Cy3-Ads for 15 min at 37°C and allowed to further incubate for the indicated periods. Then cells were fixed, permeabilized, and stained with anti-cathepsin B-specific primary antibody. The staining of primary antibody was detected with Alexa-488-conjugated secondary antibody (green), and images of cells were taken on a Leica confocal microscope. To determine colocalization of virus with cathepsin B-positive intracellular compartments, images of the same areas were acquired in red and green channels consecutively. CAR-interacting Ad5L and Ad5ΔRGD vectors do not colocalize with cathepsin B-positive compartments until 2 h postvirus infection, while CD46-interacting Ad5/35L and Ad5/35ΔRGD vectors colocalize with these cellular compartments as early as 30 min postvirus infection. Note that vectors with the penton RGD motif deletion are distributed more widely throughout the cytoplasm than RGD motif-possessing variants at earlier times postinfection. Representative fields are shown. Magnification, ×200.

The finding that penton-integrin interactions are involved in internalization of CD46-binding Ads has a number of potential consequences considering that the induction of cytokine transcription is the result, at least in part, of integrin activation and integrin-mediated signaling involving p38 MAPK and ERK1/2, and subsequent activation of NF-κB (2, 3, 18, 41) in Kupffer cells, endothelial cells, and leukocytes (18).

On the other hand, from previous studies, there are several lines of data that suggest the interaction of RGD motifs with integrins is not essential in infection of B-group fiber-containing vectors. (i) Antibodies against αv integrins that block Ad5 infection (46) do not block Ad5/35 infection (36, 37). (ii) Endosome escape (which is in part initiated by integrins) of Ad5/35 occurs much later than escape of Ad5 (35). (iii) Activation of cytokine gene expression in liver cells (a result of integrin signaling) is less pronounced after Ad5/35 than after Ad5 infection (33). Based on this, we had speculated that CD46 is not only an attachment receptor for CD46 but also mediates virus internalization (9). The discrepancy between these earlier data and the finding described in this study might have the following explanations.

(i) Importantly, the chimeric vectors used in these earlier studies have short fiber shafts (6 to 7 β-repeats), whereas in this study we used chimeric vectors that contained the long (22 β-repeats) Ad5 shaft and the Ad35 knob. CAR-interacting Ads require long fiber shafts for infections (26, 36). If the native Ad5 fiber shaft is replaced by a short fiber shaft that is less flexible, then the interaction between penton RGDs and αvβ3/5 integrins is affected due to sterical problems (48). Therefore, from our data, it cannot be concluded that chimeric vectors containing a short B-group fiber or wild-type B-group Ad serotypes (which all have short fibers) use these integrins for internalization, implying that either CD46 can mediate virus uptake or other coreceptors exist that may facilitate virus internalization upon attachment to CD46. Notably, there are also differences in the length of RGD-containing penton loops between Ad5 penton (used in our vectors) and Ad35 penton, which potentially can result in differences in integrin binding.

(ii) Other types of integrins than αv integrins might be involved in internalization/endosome escape of Ad5/35L vectors. As outlined in the introduction, RGD motifs can interact with a variety of integrins, which might explain why anti-αv integrin

antibodies had no effect on Ad5/35S infection (48). Furthermore, the expression of specific integrins varies between cell types, and this might account for the cell-type-specific differences in internalization and endosome escape that we have observed in our study.

(iii) RGD deletions affect not only interaction with integrins but might have other deleterious influence on postattachment steps of virus infections. In a recent study, we have shown that capsid integrity is critical for endosome release (32) and it cannot be excluded that mutated pentons might destabilize the capsid structure.

Although Ads with the RGD motif deleted are slightly less infectious, this apparent deficit might be compensated for by higher safety after in vivo application because they activate low-level integrin signaling, which in turn is a key player in initiating the release or production of proinflammatory cytokines and chemokines. This study contributes to a better understanding of Ad interactions with the cell and may help in developing novel, safe, and efficient Ad vectors for gene therapy applications.

ACKNOWLEDGMENTS

We thank Daniel Stone and Anuj Gaggar for helpful discussion. We are grateful to Victor Krasnykh for providing valuable materials.

This work was supported by grants from the NIH (R01 CA80192, P30 DK47754, and HL-00-008), the Cystic Fibrosis Foundation, and the Doris Duke Foundation.

REFERENCES

1. **Bai, M., B. Harfe, and P. Freimuth.** 1993. Mutations that alter an Arg-Gly-Asp (RGD) sequence in the adenovirus type 2 penton base protein abolish its cell-rounding activity and delay virus reproduction in flat cells. J. Virol. **67:**5198–5205.
2. **Borgland, S. L., G. P. Bowen, N. C. W. Wong, T. A. Libermann, and D. A. Muruve.** 2000. Adenovirus vector-induced expression of the C-X-C chemokine IP-10 is mediated through capsid-dependent activation of NF-κB. J. Virol. **74:**3941–3947.
3. **Bowen, G. P., S. L. Borgland, M. Lam, T. A. Libermann, N. C. Wong, and D. A. Muruve.** 2002. Adenovirus vector-induced inflammation: capsid-dependent induction of the C-C chemokine RANTES requires NF-kappa B. Hum. Gene Ther. **13:**367–379.
4. **Bruder, J. T., A. Appiah, W. M. Kirkman III, P. Chen, J. Tian, D. Reddy, D. E. Brough, A. Lizonova, and I. Kovesdi.** 2000. Improved production of adenovirus vectors expressing apoptotic transgenes. Hum. Gene Ther. **11:** 139–149.
5. **Carlson, C. A., D. S. Steinwaerder, H. Stecher, D. M. Shayakhmetov, and A. Lieber.** 2002. Rearrangements in adenoviral genomes mediated by inverted repeats. Methods Enzymol. **346:**277–292.
6. **Chartier, C., E. Degryse, M. Gantzer, A. Dieterlé, A. Pavirani, and M. Mehtali.** 1996. Efficient generation of recombinant adenovirus vectors by homologous recombination in *Escherichia coli*. J. Virol. **70:**4805–4810.
7. **Davison, E., R. M. Diaz, I. R. Hart, G. Santis, and J. F. Marshall.** 1997. Integrin α5β1-mediated adenovirus infection is enhanced by the integrin-activating antibody TS2/16. J. Virol. **71:**6204–6207.
8. **Davison, E., I. Kirby, J. Whitehouse, I. Hart, J. F. Marshall, and G. Santis.** 2001. Adenovirus type 5 uptake by lung adenocarcinoma cells in culture correlates with Ad5 fibre binding is mediated by alpha(v)beta1 integrin and can be modulated by changes in beta1 integrin function. J. Gene Med. **3:** 550–559.
9. **Gaggar, A., D. Shayakhmetov, and A. Lieber.** 2003. CD46 is a cellular receptor for group B adenoviruses. Nat. Med. **9:**1408–1412.
10. **Gao, W., P. D. Robbins, and A. Gambotto.** 2003. Human adenovirus type 35: nucleotide sequence and vector development. Gene Ther. **10:**1941–1949.
11. **Greber, U. F., P. Webster, J. Weber, and A. Helenius.** 1996. The role of the adenovirus protease on virus entry into cells. EMBO J. **15:**1766–1777.
12. **Hara, T., A. Kojima, H. Fukuda, T. Masaoka, Y. Fukumori, M. Matsumoto, and T. Seya.** 1992. Levels of complement regulatory proteins, CD35 (CR1), CD46 (MCP) and CD55 (DAF) in human haematological malignancies. Br. J. Haematol. **82:**368–373.
13. **Huang, S., T. Kamata, Y. Takada, Z. M. Ruggeri, and G. R. Nemerow.** 1996. Adenovirus interaction with distinct integrins mediates separate events in cell entry and gene delivery to hematopoietic cells. J. Virol. **70:**4502–4508.
14. **Kinugasa, N., T. Higashi, K. Nouso, H. Nakatsukasa, Y. Kobayashi, M. Ishizaki, N. Toshikuni, K. Yoshida, S. Uematsu, and T. Tsuji.** 1999. Expression of membrane cofactor protein (MCP, CD46) in human liver diseases. Br. J. Cancer **80:**1820–1825.
15. **Leopold, P. L., B. Ferris, I. Grinberg, S. Worgall, N. R. Hackett, and R. G. Crystal.** 1998. Fluorescent virions: dynamic tracking of the pathway of adenoviral gene transfer vectors in living cells. Hum. Gene Ther. **9:**367–378.
16. **Li, E., S. L. Brown, D. G. Stupack, X. S. Puente, D. A. Cheresh, and G. R. Nemerow.** 2001. Integrin αvβ1 is an adenovirus coreceptor. J. Virol. **75:** 5405–5409.
17. **Li, Y., R. C. Pong, J. M. Bergelson, M. C. Hall, A. I. Sagalowsky, C. P. Tseng, Z. Wang, and J. T. Hsieh.** 1999. Loss of adenoviral receptor expression in human bladder cancer cells: a potential impact on the efficacy of gene therapy. Cancer Res. **59:**325–330.
18. **Liu, Q., and D. A. Muruve.** 2003. Molecular basis of the inflammatory response to adenovirus vectors. Gene Ther. **10:**935–940.
19. **Mabit, H., M. Y. Nakano, U. Prank, B. Saam, K. Döhner, B. Sodeik, and U. F. Greber.** 2002. Intact microtubules support adenovirus and herpes simplex virus infections. J. Virol. **76:**9962–9971.
20. **Medina-Kauwe, L. K.** 2003. Endocytosis of adenovirus and adenovirus capsid proteins. Adv. Drug Delivery Rev. **55:**1485–1496.
21. **Meier, O., and U. F. Greber.** 2003. Adenovirus endocytosis. J. Gene Med. **5:** 451–462.
22. **Miyazawa, N., R. G. Crystal, and P. L. Leopold.** 2001. Adenovirus serotype 7 retention in a late endosomal compartment prior to cytosol escape is modulated by fiber protein. J. Virol. **75:**1387–1400.
23. **Miyazawa, N., P. L. Leopold, N. R. Hackett, B. Ferris, S. Worgall, E. Falck-Pedersen, and R. G. Crystal.** 1999. Fiber swap between adenovirus subgroups B and C alters intracellular trafficking of adenovirus gene transfer vectors. J. Virol. **73:**6056–6065.
24. **Mizuguchi, H., and T. Hayakawa.** 2002. Adenovirus vectors containing chimeric type 5 and type 35 fiber proteins exhibit altered and expanded tropism and increase the size limit of foreign genes. Gene **285:**69–77.
25. **Murray, K. P., S. Mathure, R. Kaul, S. Khan, L. F. Carson, L. B. Twiggs, M. G. Martens, and A. Kaul.** 2000. Expression of complement regulatory proteins—CD 35, CD 46, CD 55, and CD 59—in benign and malignant endometrial tissue. Gynecol. Oncol. **76:**176–182.
26. **Nemerow, G. R., D. A. Cheresh, and T. J. Wickham.** 1994. Adenovirus entry into host cells: a role for alpha(v) integrins. Trends Cell Biol. **4:**52–55.
27. **Rebel, V. I., S. Hartnett, J. Denham, M. Chan, R. Finberg, and C. A. Sieff.** 2000. Maturation and lineage-specific expression of the coxsackie and adenovirus receptor in hematopoietic cells. Stem Cells **18:**176–182.
28. **Roelvink, P. W., A. Lizonova, J. G. M. Lee, Y. Li, J. M. Bergelson, R. W. Finberg, D. E. Brough, I. Kovesdi, and T. J. Wickham.** 1998. The coxsackievirus-adenovirus receptor protein can function as a cellular attachment protein for adenovirus serotypes from subgroups A, C, D, E, and F. J. Virol. **72:**7909–7915.
29. **Sakurai, F., H. Mizuguchi, and T. Hayakawa.** 2003. Efficient gene transfer into human CD34+ cells by an adenovirus type 35 vector. Gene Ther. **10:** 1041–1048.
30. **Segerman, A., J. P. Atkinson, M. Marttila, V. Dennerquist, G. Wadell, and N. Arnberg.** 2003. Adenovirus type 11 uses CD46 as a cellular receptor. J. Virol. **77:**9183–9191.
31. **Shayakhmetov, D. M., C. A. Carlson, H. Stecher, Q. Li, G. Stamatoyannopoulos, and A. Lieber.** 2002. A high-capacity, capsid-modified hybrid adenovirus/adeno-associated virus vector for stable transduction of human hematopoietic cells. J. Virol. **76:**1135–1143.
32. **Shayakhmetov, D. M., Z.-Y. Li, A. Gaggar, H. Gharwan, V. Ternovoi, V. Sandig, and A. Lieber.** 2004. Genome size and structure determine efficiency of postinternalization steps and gene transfer of capsid-modified adenovirus vectors in a cell-type-specific manner. J. Virol. **78:**10009–10022.
33. **Shayakhmetov, D. M., Z.-Y. Li, S. Ni, and A. Lieber.** 2004. Analysis of adenovirus sequestration in the liver, transduction of hepatic cells, and innate toxicity after injection of fiber-modified vectors. J. Virol. **78:**5368–5381.
34. **Shayakhmetov, D. M., Z. Y. Li, S. Ni, and A. Lieber.** 2002. Targeting of adenovirus vectors to tumor cells does not enable efficient transduction of breast cancer metastases. Cancer Res. **62:**1063–1068.
35. **Shayakhmetov, D. M., Z. Y. Li, V. Ternovoi, A. Gaggar, H. Gharwan, and A. Lieber.** 2003. The interaction between the fiber knob domain and the cellular attachment receptor determines the intracellular trafficking route of adenoviruses. J. Virol. **77:**3712–3723.
36. **Shayakhmetov, D. M., and A. Lieber.** 2000. Dependence of adenovirus infectivity on length of the fiber shaft domain. J. Virol. **74:**10274–10286.
37. **Shayakhmetov, D. M., T. Papayannopoulou, G. Stamatoyannopoulos, and A. Lieber.** 2000. Efficient gene transfer into human $CD34^+$ cells by a retargeted adenovirus vector. J. Virol. **74:**2567–2583.
38. **Sirena, D., B. Lilienfeld, M. Eisenhut, S. Kalin, K. Boucke, R. R. Beerli, L. Vogt, C. Ruedl, M. F. Bachmann, U. F. Greber, and S. Hemmi.** 2004. The human membrane cofactor CD46 is a receptor for species B adenovirus serotype 3. J. Virol. **78:**4454–4462.
39. **Smith, T. A., N. Idamakanti, M. L. Rollence, J. Marshall-Neff, J. Kim, K.**

Mulgrew, G. R. Nemerow, M. Kaleko, and S. C. Stevenson. 2003. Adenovirus serotype 5 fiber shaft influences in vivo gene transfer in mice. Hum. Gene Ther. **14:**777–787.

40. **Suomalainen, M., M. Y. Nakano, S. Keller, K. Boucke, R. P. Stidwill, and U. F. Greber.** 1999. Microtubule-dependent plus- and minus end-directed motilities are competing processes for nuclear targeting of adenovirus. J. Cell Biol. **144:**657–672.
41. **Tamanini, A., R. Rolfini, E. Nicolis, P. Melotti, and G. Cabrini.** 2003. MAP kinases and NF-kappaB collaborate to induce ICAM-1 gene expression in the early phase of adenovirus infection. Virology **307:**228–242.
42. **Thorsteinsson, L., G. M. O'Dowd, P. M. Harrington, and P. M. Johnson.** 1998. The complement regulatory proteins CD46 and CD59, but not CD55, are highly expressed by glandular epithelium of human breast and colorectal tumour tissues. APMIS **106:**869–878.
43. **Tillman, B. W., T. D. de Gruijl, S. A. Luykx-de Bakker, R. J. Scheper, H. M. Pinedo, T. J. Curiel, W. R. Gerritsen, and D. T. Curiel.** 1999. Maturation of dendritic cells accompanies high-efficiency gene transfer by a CD40-targeted adenoviral vector. J. Immunol. **162:**6378–6383.
44. **Vigne, E., J. F. Dedieu, A. Brie, A. Gillardeaux, D. Briot, K. Benihoud, M. Latta-Mahieu, P. Saulnier, M. Perricaudet, and P. Yeh.** 2003. Genetic manipulations of adenovirus type 5 fiber resulting in liver tropism attenuation. Gene Ther. **10:**153–162.
45. **Vogels, R., D. Zuijdgeest, R. van Rijnsoever, E. Hartkoorn, I. Damen, M.-P. de Béthune, S. Kostense, G. Penders, N. Helmus, W. Koudstaal, M. Cecchini, A. Wetterwald, M. Sprangers, A. Lemckert, O. Ophorst, B. Koel, M. van Meerendonk, P. Quax, L. Panitti, J. Grimbergen, A. Bout, J. Goudsmit, and M. Havenga.** 2003. Replication-deficient human adenovirus type 35 vectors for gene transfer and vaccination: efficient human cell infection and bypass of preexisting adenovirus immunity. J. Virol. **77:**8263–8271.
46. **Wickham, T. J., P. Mathias, D. A. Cheresh, and G. R. Nemerow.** 1993. Integrins alpha v beta 3 and alpha v beta 5 promote adenovirus internalization but not virus attachment. Cell **73:**309–319.
47. **Wickham, T. J., E. Tzeng, L. L. Shears II, P. W. Roelvink, Y. Li, G. M. Lee, D. E. Brough, A. Lizonova, and I. Kovesdi.** 1997. Increased in vitro and in vivo gene transfer by adenovirus vectors containing chimeric fiber proteins. J. Virol. **71:**8221–8229.
48. **Wu, E., L. Pache, D. J. Von Seggern, T.-M. Mullen, Y. Mikyas, P. L. Stewart, and G. R. Nemerow.** 2003. Flexibility of the adenovirus fiber is required for efficient receptor interaction. J. Virol. **77:**7225–7235.
49. **Wu, E., S. A. Trauger, L. Pache, T. M. Mullen, D. J. von Seggern, G. Siuzdak, and G. R. Nemerow.** 2004. Membrane cofactor protein is a receptor for adenoviruses associated with epidemic keratoconjunctivitis. J. Virol. **78:**3897–3905.